

Förster resonance energy transfer with transient coherent effects

Maximilian Meyer-Mölleringhof,^{1,*} Pablo Martinez-Azcona,^{1,2,3,*} Aurélia Chenu,¹ and Tomáš Mančal^{2,†}

¹*Department of Physics and Materials Science, University of Luxembourg, L-1511 Luxembourg*

²*Faculty of Mathematics and Physics, Charles University,*

Ke Karlovu 5, CZ-121 16 Prague 2, Czech Republic

³*Currently: Walther-Meißner-Institut/Technical University of Munich/MCQST, 85748 Garching, Germany*

(Dated: February 23, 2026)

We formulate the weak intramolecular coupling Förster resonance energy transfer theory in a form suitable for calculating ultrafast non-linear response of molecular systems. We introduce a formally exact time-dependent factorization of the molecular statistical operator into the system and bath components. Combining this factorization with unperturbed environment evolution, we generalize the traditional Förster master equation for the state population probabilities into a complete master equation for the system’s reduced statistical operator. The traditional Förster theory applies in the limit where the intermolecular coupling is weak and the system-bath coupling is strong. Our technique of derivation explicitly leads to a time non-local Förster type master equation which remains valid also in the limit of vanishing system-bath coupling. The theory predicts a rapid initial coherent evolution of populations arising from a transient initial coherence-dependent term, which induces a ‘slippage’ of the initial condition that persists during subsequent rate-controlled transfer. Comparison with exact numerical results confirms the clear improvement of the present generalization over earlier formulations of the Förster theory and delineates its range of validity.

In physical chemistry and some biological disciplines, Förster resonance energy transfer (FRET) is famously used as a ruler to estimate molecular distances [1]. FRET can play this role because of its specific distance dependence owing to the dipole-dipole character of the resonance intermolecular coupling. Leaving aside the nature of the coupling, FRET theory belongs to the same family of theories as the Marcus electron transfer theory [1], both following straightforwardly from the Fermi golden rule [2]. In its original context of incoherent transfer, the rates are assumed to be slow with respect to the reorganization of the internal degrees of freedom (DOF) of the molecules and their environment. With the advent of ultrafast spectroscopy and its application to excitation energy transfer in pigment–protein complexes of photosynthesis, the Förster theory has become a robust first choice for the description of the excitation energy transfer between weakly coupled chromophores (see, e.g. [3]). In this new context, the theory had to be extended to account for transfer between weakly coupled units of mutually strongly coupled chromophores, resulting in the so-called Multichromophoric Förster theory (see e.g. [4, 5]). Also, to accommodate the ultrafast time scale, i.e., to relax the condition of fast internal reorganization, the Nonequilibrium Förster theory was developed in ref. [6], in which the bath reorganization dynamics is accounted for.

Ultrafast laser pulse excitation of a multichromophoric system leads inevitably to coherent initial state. No systematic treatment of decoherence is, however, provided within the traditional Förster theory, and the rates of decoherence are typically

postulated phenomenologically to satisfy a strict density matrix positivity condition embedded, e.g., within the Lindblad form [7, 8]. This requires coherence element $\rho_{ab} = \langle a|\hat{\rho}|b\rangle$ to decay with one-half of the depopulation rates of each of the states $|a\rangle$ and $|b\rangle$ (the *one-half rule*). In this Letter, we introduce a general technique to derive an equation of motion (EM) for the reduced density matrix (RDM) of an open quantum system, enabling us to derive a complete theory of Förster type that also rigorously includes decoherence dynamics. This makes the proposed theory truly suitable for the description of ultrafast optical experiments. The technique is based on an exact decomposition of the composite statistical operator into the system and bath components, together with a physically motivated time-dependent *ansatz* for the bath components. After laying out the theory for a general multistate molecular open quantum system, we study the dynamics of a donor–acceptor system and compare the results obtained from different types of master equations to the numerically exact solution of the Hierarchical Equations of Motion (HEOM) [9]. We identify the region of parameters in which different versions of the Förster theory can be considered valid. Most notably, we find a very high degree of agreement between the present generalized Förster theory and the exact dynamics during the initial transient time window of coherent dynamics. In contrast to the traditional weak intramolecular coupling theories, our formulation is well-defined also in the limit of the vanishing system–bath coupling for any value of the intramolecular coupling.

The system.— Let us consider the Frenkel exciton Hamiltonian found in the theory of protein-embedded molecular aggregates (see e.g. [10, 11]). We divide it into four convenient components, $\hat{H} = \hat{H}_S + \hat{H}_B + \hat{V}_{S-S} + \hat{V}_{S-B}$. The molecular system, \hat{H}_S , is made up

* These authors contributed equally to this work

† tomas.mancal@matfyz.cuni.cz

of N two-level molecules, $\hat{H}_a = \epsilon_a^{(g)} |g_a\rangle\langle g_a| + \epsilon_a^{(e)} |e_a\rangle\langle e_a|$, where $|g_a\rangle$ and $|e_a\rangle$ represent the molecular electronic ground and excited states, respectively. We consider the single-excitation approximation, as appropriate for energy-transfer problems in photosynthesis, and denote the collective single-excitation states $|a\rangle = \prod_{b \neq a}^N |g_b\rangle |e_a\rangle$ and ground state $|g\rangle = \prod_a |g_a\rangle$. The system Hamiltonian then reads as $\hat{H}_S = \epsilon_g |g\rangle\langle g| + \sum_{a=1}^N \epsilon_a |a\rangle\langle a|$, with $\epsilon_a = \epsilon_a^{(e)}$ and $\epsilon_g = \sum_a \epsilon_g^{(a)}$ set to zero. Electronic transitions on individual molecules interact through electrostatic resonance interaction $\hat{V}_{S-S} = \sum_{ab} J_{ab} |a\rangle\langle b|$. Their energy gaps are modulated by the pure dephasing interaction with the protein DOF and the intramolecular vibrational modes that together form their environment.

When the molecules are in their electronic ground states, the environment (also referred to as the bath) is represented by an infinite set of harmonic modes with the Hamiltonian $\hat{H}_B = \frac{1}{2} \sum_{ak} \hbar \omega_{a,k} (\hat{p}_{a,k}^2 + \hat{q}_{a,k}^2)$. Upon electronic excitation, the pure dephasing interaction between electronic and bath DOF amounts to a potential energy surface shift $d_{b,k}$ such that the bath Hamiltonian experienced by the electronic excited state reads $\hat{H}_B^{(a)} = \frac{1}{2} \sum_{bk} \hbar \omega_{b,k} (\hat{p}_{b,k}^2 + (\hat{q}_{b,k} - \delta_{ab} d_{b,k})^2)$. The Hamiltonian $\hat{H}_0 = (\epsilon_g + \hat{H}_B) |g\rangle\langle g| + \sum_a (\epsilon_a + \hat{H}_B^{(a)}) |a\rangle\langle a|$ can thus be described as independent levels coupled to different baths [12, 13], or equivalently, as $\hat{H}_0 = \hat{H}_S + \hat{H}_B + \hat{V}_{S-B}$, where the effective interaction $\hat{V}_{S-B} = \sum_a \hat{X}_a |a\rangle\langle a|$ is given by the so-called energy-gap operator $\hat{X}_a = -\sum_k \hbar \omega_{a,k} d_{a,k} \hat{q}_{a,k}$, linear in the bath coordinates. The excited state energies of the aggregate molecules are each renormalized by the so-called reorganization energy $\lambda_a = \frac{1}{2} \sum_k \hbar \omega_{a,k} d_{a,k}^2$ and $\hat{H}_B^{(a)} = \hat{H}_B + \lambda_a + \hat{X}_a$.

The system–bath interaction is characterized by the so-called energy gap correlation functions (EGCFs), $C_{ab}(t) = \text{Tr}_B \{ \hat{X}_a(t) \hat{X}_b \hat{w}_{eq} \}$, where \hat{w}_{eq} is the statistical operator for the bath at thermal equilibrium with respect to the molecular electronic ground state. The function $C_{ab}(t)$ measures the correlations of energy gap fluctuations. For photosynthetic systems, the fluctuations on different molecules are mostly uncorrelated, and $C_{ab}(t) = C_{aa}(t) \delta_{ab}$ is a good approximation [14, 15]. The first and second integrals of $C_{ab}(t)$, i.e. $\dot{g}_{ab}(t) = \int_0^t d\tau C_{ab}(\tau)$ and the line-shape function $g_{ab}(t) = \int_0^t d\tau \int_0^\tau d\tau' C_{ab}(\tau')$, play an important role in the theory of spectroscopy and will be used to express our results in this paper.

General second-order equation of motion.— We will now present the equations governing the time evolution of the open quantum system’s RDM $\hat{\rho}(t)$. We start with the full system–bath statistical operator $\hat{W}(t)$ that evolves according to the Liouville–von Neumann equation, $\frac{\partial}{\partial t} \hat{W}(t) = -\frac{i}{\hbar} [\hat{H}, \hat{W}(t)]$. We divide the total Hamiltonian as $\hat{H} = \hat{H}_0 + \hat{V}$, where \hat{V} is a suitably chosen weak perturbation. In the context of Förster resonance energy transfer [16, 17], the weak interaction is between the states of the system, i. e., $\hat{V} = \hat{V}_{S-S}$. The reference

Hamiltonian \hat{H}_0 cannot be decomposed into a sum of \hat{H}_S and \hat{H}_B , however, its form still allows us to evaluate the unperturbed dynamics exactly. Using the reference evolution operator $\hat{U}_0(t) = e^{-\frac{i}{\hbar} \hat{H}_0 t}$, we derive the following identity (see SI) which forms the basis of our theoretical methodology:

$$\begin{aligned} \frac{\partial}{\partial t} \hat{W}(t) &= -\frac{i}{\hbar} [\hat{V}, \hat{U}_0(t) \hat{W}(0) \hat{U}_0^\dagger(t)] - \frac{i}{\hbar} [\hat{H}_0, \hat{W}(t)] \\ &\quad - \frac{1}{\hbar^2} \int_0^t d\tau [\hat{V}, \hat{U}_0(\tau) [\hat{V}, \hat{W}(t-\tau)] \hat{U}_0^\dagger(\tau)]. \end{aligned} \quad (1)$$

This equation of motion (EM) is exact and it is nonlocal in time. Tracing over the bath DOF yields the dynamics relevant to the system of interest in terms of the RDM $\hat{\rho}(t) = \text{Tr}_B \{ \hat{W}(t) \}$. However, since $\hat{W}(t)$ is surrounded by bath operators, this last step is the main challenge — and the central topic of the present letter. It results in an approximate equation for the RDM that closely follows the general form:

$$\frac{\partial}{\partial t} \hat{\rho}(t) = \hat{I}(t) - i\mathcal{L}(t) \hat{\rho}(t) - \int_0^t d\tau \mathcal{M}(t, \tau) \hat{\rho}(t - \tau). \quad (2)$$

Here, $\hat{I}(t)$ is an operator depending on the initial condition $\hat{\rho}(0)$, $\mathcal{L}(t)$ is the Liouville superoperator capturing the unitary evolution and the decoherence due to pure dephasing interaction with the environment—with a time dependence that originates from the time-evolution of the bath state—and $\mathcal{M}(t, \tau)$ is the memory kernel superoperator, which captures the influence of the past on the present RDM.

The bath state ansatz.— Our derivation of a general equation of motion relies on the observation that the total statistical operator can be factorized as

$$\hat{W}(t) = \sum_{ab} \rho_{ab}(t) \hat{w}_{ab}(t) |a\rangle\langle b|, \quad (3)$$

where the states $\{|a\rangle\}$ form a relevant physical basis for the system of interest which is taken to be the site basis, $\rho_{ab}(t) = \langle a | \hat{\rho}(t) | b \rangle = \text{Tr}_B \{ \hat{W}_{ab}(t) \}$, and where we have defined the relative bath state operators $\hat{w}_{ab}(t) \equiv \hat{W}_{ab}(t) / \rho_{ab}(t)$. To be able to employ the factorization, Eq. (3), we need to approximate the relative bath operator $\hat{w}_{ab}(t)$ in a suitable way. The reference dynamics of perturbation theory is the evolution dictated by the Hamiltonian \hat{H}_0 alone. Taking such a zero’s order (in V_{S-S}) evolution of the bath as the reference corresponds to the following time-dependent approximation for its state operators, relative to the electronic states:

$$\hat{w}_{ab}(t) = \frac{\hat{u}_a(t) \hat{w}_{eq} \hat{u}_b^\dagger(t)}{\text{Tr}_B \{ \hat{u}_a(t) \hat{w}_{eq} \hat{u}_b^\dagger(t) \}}. \quad (4)$$

We will take this normalized density operator as an ansatz for the bath. Here, the evolution operators $\hat{u}_a(t) \equiv e^{-i\hat{H}_B^{(a)} t / \hbar}$ describe the bath evolution on the

potential energy surface (PES) of the electronic state $|a\rangle$ and $\hat{w}_{\text{eq}} = e^{-\beta\hat{H}_B}/Z$ is the density operator of the bath in equilibrium with respect to the electronic ground state, $Z = \text{Tr}_B(e^{-\beta\hat{H}_B})$ being the bath partition function. Although Eq. (4) is a zeroth-order approximation, it conveniently corresponds to the bath state operators implicit to the non-equilibrium Förster theory [6].

Equations of motion in Förster limit.— We now use the approximation, Eq. (4), to derive the equations of motion for all elements of the RDM for a system of weakly coupled molecules. In the following, we calculate all the expected components of the master equation, Eq. (2), using the cumulant expansion. The details of the derivations can be found in the SI.

(i) *Initial term:* The first term on the r.h.s. of Eqs. (1) and (2) depends only on the initial state of the total system. We assume that the system is initially excited by a spectrally broad laser pulse. In the Condon approximation, this corresponds to $\hat{W}(0) = \hat{\rho}(0)\hat{w}_{\text{eq}}$, with $\hat{\rho}(0)$ a possibly coherent superposition of electronic excited states. Such an initial condition is required for calculating non-linear optical response functions. The initial term can be expressed compactly by defining the dephasing operator $\hat{D}(t) \equiv \sum_{ab} D_{ab}(t) |a\rangle\langle b|$, with the elements

$$\begin{aligned} D_{ab}(t) &= \text{Tr}_B\{\hat{u}_b^\dagger(t)\hat{u}_a(t)\hat{w}_{\text{eq}}\}e^{-i\omega_{ab}t} \\ &= e^{-g_{aa}(t)-g_{bb}^*(t)+2\text{Re}(g_{ab}(t))-i\omega_{ab}t}, \end{aligned} \quad (5)$$

and the so-called Hadamard (element-wise) product denoted by \circ . We obtain

$$\hat{I}(t) = -\frac{i}{\hbar}[\hat{V}_{S-S}, \hat{D}(t) \circ \hat{\rho}(0)]. \quad (6)$$

This ‘initial term’ connects the initial site populations with the coherence elements of the reduced statistical operator, and *vice versa*. As expected, it redistributes the population during the time window in which it is non-zero, while keeping their total unchanged since $\sum_a I_{aa}(t) = 0$.

(ii) *Hamiltonian term:* The second term on the r.h.s. of Eqs. (1) and (2), is defined as the commutator of the total statistical operator $\hat{W}(t)$ with the Hamiltonian \hat{H}_0 . This can be evaluated using our ansatz for the bath, Eq. (4), as detailed in the SI, and written as

$$\mathcal{L}(t)\hat{\rho}(t) = \hat{\Omega}(t) \circ \hat{\rho}(t), \quad (7)$$

where the elements of the $\hat{\Omega}(t)$ operator are defined as

$$\begin{aligned} \Omega_{ab}(t) &= i\dot{D}_{ab}(t)/D_{ab}(t) \\ &= \omega_{ab} - i\dot{g}_{aa}(t) - i\dot{g}_{bb}^*(t) + 2i\text{Re}\dot{g}_{ab}(t). \end{aligned} \quad (8)$$

This result reproduces the pure dephasing dynamics of two uncoupled molecules. We assume $g_{ab}(t) = 0$ for $a \neq b$ in all calculations. There is no contribution of the Hamiltonian term to the population dynamics.

(iii) *Memory kernel:* The last terms of Eqs. (1) and (2) are the convolutions of the statistical operator with

a memory kernel \mathcal{M} . The kernel contains two nested commutators of the total statistical operator with the interaction operators \hat{V} , i.e. four terms in total. Each term represents two actions of the interaction operator, at time $t - \tau$ and t . The kernel contributions can be evaluated by applying the factorization, Eq. (3), to the total statistical operator and tracing the whole expression over the bath DOF. The kernel will be expressed in terms of the bath evolution correlators $F_{cd}^{ad}(t, \tau) \equiv \text{Tr}_B\{\hat{u}_a(\tau)\hat{w}_{cd}(t - \tau)\hat{u}_d^\dagger(\tau)\}e^{-i\omega_{ad}\tau}$, representing the history of bath time-evolution on different PES starting from the RDM element ρ_{cd} . Taking the approximate form, Eq. (4), for the bath allows to evaluate the bath correlator as $F_{cd}^{ad}(t, \tau) \approx f_{cd}^{ad}(t, \tau)e^{-i\omega_{ad}\tau}$ with:

$$f_{cd}^{ad}(t, \tau) = \frac{\text{Tr}_B\{\hat{u}_a(\tau)\hat{u}_c(t - \tau)\hat{w}_{eq}\hat{u}_d^\dagger(t)\}}{\text{Tr}_B\{\hat{u}_c(t - \tau)\hat{w}_{eq}\hat{u}_d^\dagger(t - \tau)\}}. \quad (9)$$

The bath correlators fully characterize all integration kernels considered here, and can be evaluated using the cumulant expansion technique. In order to avoid errors in this straightforward but tedious calculation, we evaluate Eq. (9) using a symbolic module of our software package *Quantarhei* [18] which is based on Sympy [19]. This yields (see SI for details)

$$\begin{aligned} f_{cd}^{ad}(t, \tau) &= e^{-g_{aa}(\tau) - g_{dd}^*(t) + g_{dd}^*(t - \tau) + g_{da}(\tau) + g_{da}^*(t)} \\ &\times e^{-g_{da}^*(t - \tau) - g_{ac}(t) + g_{ac}(\tau) + g_{ac}(t - \tau)} \\ &\times e^{-g_{dc}(\tau) + g_{dc}(t) - g_{dc}(t - \tau)}. \end{aligned} \quad (10)$$

The approximate correlator $f_{cd}^{ad}(t, \tau)$ conserves an important behavior of $F_{cd}^{ad}(t, \tau)$, namely that $F_{ca}^{aa}(t, \tau) = f_{ca}^{aa}(t, \tau) = 1$, for all values of c and a . An important special case is the expression where the diagram starts with $c = d$, i.e. $f_{cc}^{ac}(t, \tau) = e^{-g_{aa}(\tau) - g_{cc}(\tau) - ih_{cc}(t, \tau)}$, which appears in the expression for the population rates. Here, we defined $h_{cc}(t, \tau) = 2\text{Im}[g_{cc}(t - \tau) - g_{cc}(t)]$. With the expression, Eq. (10), for the correlators, Eq. (9), we can construct all the matrix elements entering the equation of motion for the reduced statistical operator.

Non-equilibrium Förster rates in a donor-acceptor system — For a simple molecular donor-acceptor system ($N = 2$), all terms of Eq. (1) can be easily written out and traced over the bath using the results and definitions listed above. We obtain EM for populations $\rho_{11}(t)$ and $\rho_{22}(t)$ that are independent of the coherence elements $\rho_{12}(t)$ and *vice versa*. The dimer problem is therefore inherently secular, with the exception of the dependence on the initial condition. The population part of the EM has the form

$$\begin{aligned} \frac{\partial}{\partial t}\rho_{11}(t) &= -\frac{i}{\hbar}J_{12}[D_{21}(t)\rho_{21}(0) - \rho_{12}(0)D_{12}(t)] \\ &- \frac{|J_{12}|^2}{\hbar^2}2\text{Re}\int_0^t d\tau e^{-g_{22}(\tau) - g_{11}(\tau) - ih_{11}(t, \tau) - i\omega_{21}\tau} \rho_{11}(t - \tau) \\ &+ \frac{|J_{12}|^2}{\hbar^2}2\text{Re}\int_0^t d\tau e^{-g_{11}(\tau) - g_{22}(\tau) - ih_{22}(t, \tau) - i\omega_{12}\tau} \rho_{22}(t - \tau). \end{aligned} \quad (11)$$

Eq. (11) is time-non-local and can be approximately time-localized by approximating $\rho_{nn}(t - \tau) \approx \rho_{nn}(t)$. The resulting relaxation rates correspond exactly to the non-equilibrium Förster rates in Ref. [6]. Moreover, as the non-equilibrium Förster rates asymptotically converge to the standard Förster rates the present theory leads to the canonical equilibrium between the populations of the states $|1\rangle$ and $|2\rangle$ at $t \rightarrow \infty$. The initial condition term is transient due to the presence of the dephasing term $D_{ab}(t)$ of Eq. (5) and it has already been identified in Ref. [6]. Here, we identify its crucial role for the short time dynamics.

Decoherence dynamics.— In addition to the rate theory, our formulation also provides an expression for the evolution of coherences. Due to the analytical properties of the correlators, we have $f_{ca}^{aa} = 1$, and the integral term of the equation lacks any dependence on the bath DOF. This gives the equation for the dephasing of coherence in the form of

$$\frac{\partial}{\partial t} \rho_{12}(t) = -\frac{i}{\hbar} J_{12} [\rho_{22}(0) - \rho_{11}(0)] - i\omega_{12} \rho_{12}(t) \quad (12)$$

$$- [\dot{g}_{11}(t) + \dot{g}_{22}^*(t)] \rho_{12}(t) - \frac{4i|J_{12}|^2}{\hbar^2} \int_0^t d\tau \text{Im}(\rho_{12}(\tau)).$$

To our knowledge, this is an entirely new form of dephasing equation valid in the Förster regime of energy transfer. Although Eq. (12) as a whole is not exact, the derivation of its surprising integral term does not contain any approximations. Eq. (12) remains valid even when the interaction with the bath is absent. By itself, it does not introduce any new dephasing. This implies that in the Förster regime of energy transfer, no transfer rate associated dephasing is present, and *the one-half rule does not apply*. Despite its integral form, the numerical solution of Eq. (12) is not more demanding than the solution of the time-local equation because the integral needs to be only incrementally updated in each time step. The non-integral terms of Eq. (12) have constant factors at large values of t . If the coherence is to become stationary as the system reaches equilibrium, the imaginary part of the coherence elements has to become zero. A non-zero constant imaginary part of the coherence element would lead to an ever increasing integral term and would contradict stationarity at the equilibrium.

Quality of the generalized Förster theory.— To verify that our methodology, denoted here as the generalized Förster theory (gFT), indeed improves on the standard Förster theory [10] and even its recent non-equilibrium version (neqFT) [6], we compare the results of Eqs. (11) and (12) with the exact solution of the corresponding dynamics of HEOM calculated using QuTiP [20]. We model the environment with a Drude-Lorentz spectral density, characterized by the reorganization energy λ , which is a measure of the system-bath coupling strength, and the bath correlation time t_c . Using the Padé expansion, we obtain the correlation function $C_{ab}(t)$, which, by integration, provides $\dot{g}_{ab}(t)$ and $g_{ab}(t)$ as mentioned above. For all the following results, we set $T = 277\text{K}$. As a compar-

ative metric for the results, we choose the trace distance $T(\hat{\rho}, \hat{\sigma}) = \frac{1}{2} \text{Tr} \left(\sqrt{(\hat{\rho} - \hat{\sigma})^\dagger (\hat{\rho} - \hat{\sigma})} \right)$ to define the maximum error with respect to HEOM over a time-interval $\varepsilon = \max_{t \in [t_0, t_1]} T(\hat{\rho}^{\text{neqFT}}(t), \hat{\rho}^{\text{HEOM}}(t))$. We split it into its population part ε_{pop} and its coherence part ε_{coh} (see SI). The neqFT time-dependent relaxation rates quickly converge to standard time-independent Förster rates, and correspondingly, we chose neqFT as the most favorable representation of the standard Förster energy transfer theory. We assume that it lacks the initial condition term. The gFT which contains the initial condition term can be time-localized yielding the neqFT rates. For the purpose of this paper, therefore, the time-localized gFT differs from the neqFT only by the presence of the initial condition term.

In Fig. 1(a,b), we present typical population dynamics after a fully coherent initial condition $\rho_{11}(0) = 0.4$, $\rho_{22}(0) = 0.6$ and $\rho_{12}(0) = \sqrt{\rho_{11}(0)\rho_{22}(0)}$ calculated by HEOM, gFT and neqFT. The parameters are listed in the figure caption. We notice that neqFT lacks the initial fast population dynamics. This is especially clear at a large energy gap of $\Delta E = 300 \text{ cm}^{-1}$, exemplified in Fig. 1(b). In Fig. 1(c-e) we present the maximum ε_{pop} for gFT [including also its time-localized version (d)] and neqFT compared to HEOM, respectively, for a wide range of system parameters λ and J at short times ($t < t_c$). The parameter region where gFT agrees with HEOM in the window of short times, i.e. when dynamics is influenced by initial coherence, far exceeds the expected region of weak resonance coupling. The quality of agreement between gFT and HEOM depends, to some extent, only on the coupling J . Comparing results in Fig. 1(d) and (e), shows that this is largely due to time non-local effects. This is a clear improvement over neqFT, Fig. 1(c), which shows noticeable disagreement with the results of HEOM. For short time dynamics, combination of time non-local equations and the initial term yields significantly better results than the presence of the initial term alone. After the fast transient dynamics ($t > t_c$), all versions of the dynamics are clearly rate dominated, and the gFT gives a rate that agrees very well with the effective rate corresponding to the HEOM dynamics. For a good agreement of the dynamics in this time window, it is however crucial that the dynamics agree during the short time window. As presented in Fig. 1(f), in the intermediate time window, we find that the quality of the gFT dynamics depends non-linearly on both λ and J with increasing λ improving the agreement for any value of J . In the photosynthetic FMO complex that clearly shows signs of exciton delocalization, the maximum couplings are $J \sim 130 \text{ cm}^{-1}$, depending on the parameterization [21], while the typical value is around 20 or 30 cm^{-1} . The energy gaps are up to 400 cm^{-1} . Therefore, gFT would perform rather well in FMO for short and intermediate times with $\varepsilon_{pop} < 0.04$ for typical values of resonance coupling and reorganization energy. Note that, remarkably, the intermediate time error of gFT is com-

parable, and even smaller, than the short time error of the alternative Förster theories.

In Fig. 2, we present ε_{coh} for the same range of parameters as discussed for the populations. It is clear that the gFT describes the coherence evolution much less accurately than the populations, especially at longer times. This is to be expected for systems showing the effect of electronic state delocalization which translates into non-zero real values of long time coherence elements of the RDM when represented the basis of local molecular states. This effect is not captured by the present theory at all. The detailed analysis of the coherence evolutions can be found in the SI, confirming the agreement of the gFT and HEOM for the coherence evolution at very short times, good agreement of the imaginary part of the coherence elements, and the failure of the gFT to capture of the non-zero real parts of the RDM at long times. Interestingly, the error depends non-trivially on the relative strength of the resonance and the system-bath couplings and is pronounced especially at larger energy gaps. The description of coherence by gFT is very good for both the limits of small λ and small J .

Conclusions — In this letter, we derived a complete second-order reduced density matrix theory valid in the parameter regime characterized by the weak intermolecular coupling and the strong system–bath coupling (the Förster theory regime). We found that coherence in the initial condition rapidly redistributes populations and thus causes a lasting mismatch between exact dynamics and the standard Förster theory. Our theory provides a novel form of decoherence equation that accurately captures the initial coherent dynamics of the system for the parameter range exceeding the weak resonance coupling regime. Besides the weak coupling, the present theory is also exact for vanishing system-bath coupling and an arbitrary strength of resonance coupling. We find that all variants of the Förster theories predict similar energy transfer rates that compare well to the dynamics obtained from HEOM in an extensive region of parameters. However, capturing the initial coherent dynamics correctly, by including the initial correlation term and time-non-local form of the relaxation, is crucial for agreement with the exact dynamics, even in propagation times when the dynamics is dominated by the rate process. The technique we introduced in this letter for deriving master equations for the reduced density matrix can be combined with better approximations to the bath evolution to further improve the agreement with exact dynamics and to adapt Förster theory for different spectroscopic situations including multi-dimensional spectroscopies.

ACKNOWLEDGMENTS

We thank Alessandro Manacorda and Veljko Jankovic for insightful discussions and Neill Lambert for helping with the HEOM simulations. This work was partially funded by the Luxembourg National Research Fund

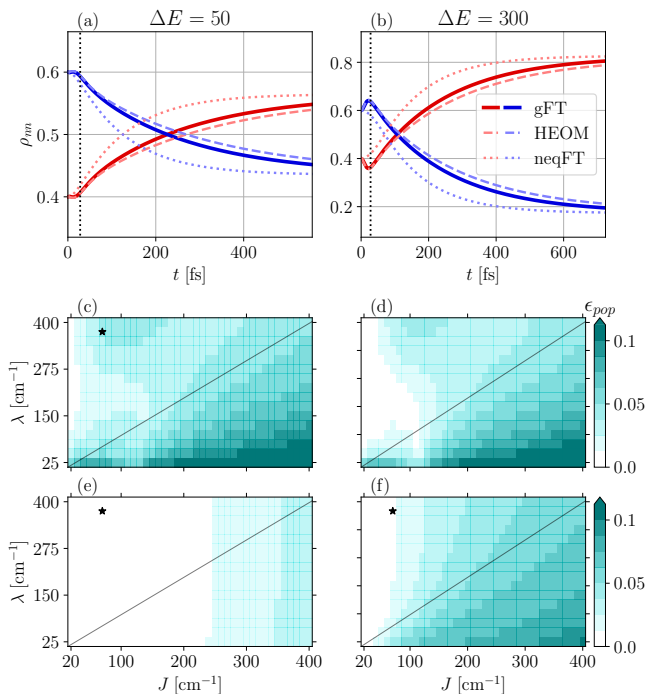


FIG. 1. (a,b) Evolution of populations in a donor-acceptor system as obtained from gFT, Eqs. (11) and (12) (solid lines), from the exact numerical results using HEOM (dashed lines) and neqFT (dotted lines). The dashed black line indicates the bath correlation time $t_c = 30$ fs. (c-e) Short time ($t < t_c$) evaluation of maximum population-only trace distance ε_{pop} for a range of λ and J . The results from HEOM are compared with (c) neqFT, (d) time localized gFT and (e) full gFT. (f) The distance ε_{pop} for gFT and HEOM calculated density matrices at intermediate times ($t_c < t < t_s$, where t_s indicates the time at which equilibrium is reached). All diagrams (c-f) are for $\Delta E = 50 \text{ cm}^{-1}$ with the star indicating the system parameters for the evolutions presented in (a,b): $J = 70 \text{ cm}^{-1}$, $\lambda = 325 \text{ cm}^{-1}$. The gray line indicates $J = \lambda$.

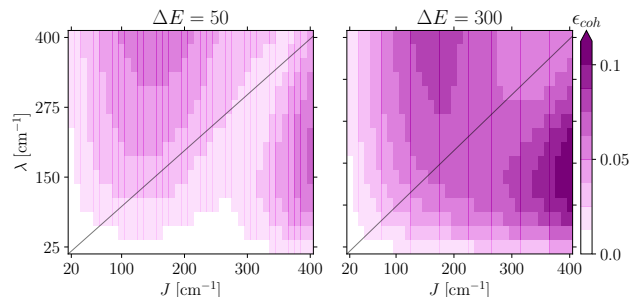


FIG. 2. Short time ($t < t_c$) evaluation of coherence-only trace distance ε_{coh} in a donor-acceptor system as obtained from the derived EM Eqs. (11), (12) and HEOM at two different energy gaps ΔE . At the gray line $J = \lambda$.

(FNR, Attract grant 15382998). TM acknowledges fund-

ing support from the Czech Science Foundation via grant no. 22-26376S.

-
- [1] C. R. Cantor and P. R. Schimmel, *Biophysical Chemistry, Part II* (W. H. Freeman and co., New York, 2001).
- [2] V. May and O. Kühn, *Charge and Energy Transfer Dynamics in Molecular Systems* (Wiley-VCH, Berlin, 2001).
- [3] D. Zigmantas, E. L. Read, T. Mančal, T. Brixner, A. T. Gardiner, R. J. Cogdell, and G. R. Fleming, Two-dimensional electronic spectroscopy of the B800–B820 light-harvesting complex, *Proceedings of the National Academy of Sciences* **103**, 12672 (2006).
- [4] H. Sumi, Theory on rates of excitation-energy transfer between molecular aggregates through distributed transition dipoles with application to the antenna system in bacterial photosynthesis, *J. Phys. Chem. B* **103**, 252–260 (1999).
- [5] S. Jang, M. D. Newton, and R. J. Silbey, Multichromophoric Förster resonance energy transfer, *Phys. Rev. Lett.* **92**, 218301 (2004).
- [6] J. Seibt and T. Mančal, Ultrafast energy transfer with competing channels: Non-equilibrium Förster and Modified Redfield theories, *The Journal of Chemical Physics* **146**, 174109 (2017).
- [7] G. Lindblad, On the generators of quantum dynamical semigroups, *Comm. Math. Phys.* **48**, 119 (1976).
- [8] H.-P. Breuer and F. Petruccione, *The Theory of Open Quantum Systems* (Oxford University Press, 2007).
- [9] A. Ishizaki and G. R. Fleming, Unified treatment of quantum coherent and incoherent hopping dynamics in electronic energy transfer: Reduced hierarchy equation approach, *J. Chem. Phys.* **130**, 234111 (2009).
- [10] L. Valkunas, D. Abramavičius, and T. Mančal, *Molecular Excitation Dynamics and Relaxation: Quantum Theory and Spectroscopy* (Wiley-VCH, Weinheim, 2013).
- [11] T. Renger and F. Müh, *Understanding photosynthetic light-harvesting: A bottom up theoretical approach* (2013).
- [12] G. D. Mahan, *Many-Particle Physics*, 3rd ed. (Kluwer Academic Publishers, 2000).
- [13] A. Chenu, S.-Y. Shiao, and M. Combescot, Two-level system coupled to phonons: Full analytical solution, *Phys. Rev. B* **99**, 014302 (2019).
- [14] C. Olbrich, J. Strümpfer, K. Schulten, and U. Kleinekathöfer, Quest for spatially correlated fluctuations in the FMO light-harvesting complex, *J. Phys. Chem. B* **115**, 758 (2011).
- [15] T. Renger, A. Klinger, F. Steinecker, M. S. A. Busch, J. Numata, and F. Müh, Normal mode analysis of the spectral density of the fenna-matthews-olson light-harvesting protein: How the protein dissipates the excess energy of excitons, *Journal of Physical Chemistry B* **116**, 14565 (2012).
- [16] T. Förster, Energiewanderung und Fluoreszenz, *Die Naturwissenschaften* **33**, 166 (1946).
- [17] T. Förster, Zwischenmolekulare Energiewanderung und Fluoreszenz, *Annalen der Physik* **437**, 55 (1948).
- [18] T. Mančal and contributors, *Quantarhei: Open quantum-system simulator for molecular aggregates*, Quantarhei Development Team (2025), commit/tag or release version used for simulations.
- [19] A. Meurer, C. P. Smith, M. Paprocki, O. Čertík, S. B. Kirpichev, M. Rocklin, A. Kumar, S. Ivanov, J. K. Moore, S. Singh, T. Rathnayake, S. Vig, B. E. Granger, R. P. Müller, F. Bonazzi, H. Gupta, S. Vats, F. Johansson, F. Pedregosa, M. J. Curry, A. R. Terrel, Š. Roučka, A. Saboo, I. Fernando, S. Kulal, R. Cimrman, and A. Scopatz, Sympy: symbolic computing in python, *PeerJ Computer Science* **3**, e103 (2017).
- [20] N. Lambert, E. Giguère, P. Menczel, B. Li, P. Hopf, G. Suárez, M. Gali, J. Lishman, R. Gadhvi, R. Agarwal, A. Galicia, N. Shammah, P. Nation, J. Johansson, S. Ahmed, S. Cross, A. Pitchford, and F. Nori, Qutip 5: The quantum toolbox in python, *Physics Reports* **1153**, 1 (2026).
- [21] J. Adolphs and T. Renger, How proteins trigger excitation energy transfer in the FMO complex of green sulfur bacteria, *Biophys. J.* **91**, 2778 (2006).